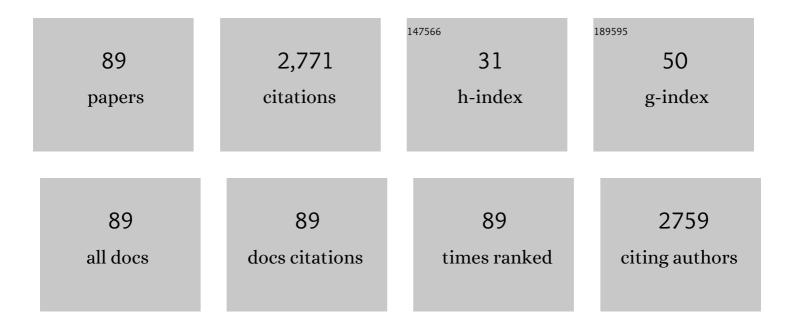
Liliana de Campo

List of Publications by Year in descending order

Source: https://exaly.com/author-pdf/9478948/publications.pdf Version: 2024-02-01



#	Article	IF	CITATIONS
1	Emulsified Microemulsions and Oil-Containing Liquid Crystalline Phases. Langmuir, 2005, 21, 569-577.	1.6	241
2	Reversible Phase Transitions in Emulsified Nanostructured Lipid Systems. Langmuir, 2004, 20, 5254-5261.	1.6	222
3	Oil-Loaded Monolinolein-Based Particles with Confined Inverse Discontinuous Cubic Structure (Fd3m). Langmuir, 2006, 22, 517-521.	1.6	162
4	Control of the Internal Structure of MLO-Based Isasomes by the Addition of Diglycerol Monooleate and Soybean Phosphatidylcholine. Langmuir, 2006, 22, 9919-9927.	1.6	125
5	Crystallography of dispersed liquid crystalline phases studied by cryo-transmission electron microscopy. Journal of Microscopy, 2006, 221, 110-121.	0.8	117
6	Performance and characteristics of the BILBY time-of-flight small-angle neutron scattering instrument. Journal of Applied Crystallography, 2019, 52, 1-12.	1.9	90
7	Tunable Biomimetic Hydrogels from Silk Fibroin and Nanocellulose. ACS Sustainable Chemistry and Engineering, 2020, 8, 2375-2389.	3.2	84
8	Five-component food-grade microemulsions: structural characterization by SANS. Journal of Colloid and Interface Science, 2004, 274, 251-267.	5.0	71
9	Design and performance of the variable-wavelength Bonse–Hart ultra-small-angle neutron scattering diffractometer KOOKABURRA at ANSTO. Journal of Applied Crystallography, 2018, 51, 1-8.	1.9	68
10	Evolution of the Interfacial Structure of a Catalyst Ink with the Quality of the Dispersing Solvent: A Contrast Variation Small-Angle and Ultrasmall-Angle Neutron Scattering Investigation. ACS Applied Materials & Interfaces, 2019, 11, 9934-9946.	4.0	65
11	BILBY: Time-of-Flight Small Angle Scattering Instrument. Neutron News, 2016, 27, 9-13.	0.1	59
12	Tough Photocrosslinked Silk Fibroin/Graphene Oxide Nanocomposite Hydrogels. Langmuir, 2018, 34, 9238-9251.	1.6	54
13	Self-Assembly of Long-Chain Betaine Surfactants: Effect of Tailgroup Structure on Wormlike Micelle Formation. Langmuir, 2018, 34, 970-977.	1.6	52
14	The effects of small molecule organic additives on the self-assembly and rheology of betaine wormlike micellar fluids. Journal of Colloid and Interface Science, 2019, 534, 518-532.	5.0	51
15	Structural characterization of five-component food grade oil-in-water nonionic microemulsions. Physical Chemistry Chemical Physics, 2004, 6, 1524-1533.	1.3	48
16	Robust and Tunable Hybrid Hydrogels from Photo-Cross-Linked Soy Protein Isolate and Regenerated Silk Fibroin. ACS Sustainable Chemistry and Engineering, 2019, 7, 9257-9271.	3.2	44
17	Influence of Vitamin E Acetate and Other Lipids on the Phase Behavior of Mesophases Based on Unsaturated Monoglycerides. Langmuir, 2013, 29, 8222-8232.	1.6	42
18	Effect of NaCl and CaCl2 concentration on the rheological and structural characteristics of thermally-induced quinoa protein gels. Food Hydrocolloids, 2022, 124, 107350.	5.6	42

#	Article	IF	CITATIONS
19	Chelating phytanyl-EDTA amphiphiles: self-assembly and promise as contrast agents for medical imaging. Soft Matter, 2010, 6, 5915.	1.2	41
20	Bulk properties of aqueous graphene oxide and reduced graphene oxide with surfactants and polymers: adsorption and stability. Physical Chemistry Chemical Physics, 2018, 20, 16801-16816.	1.3	41
21	Rheological and structural characterization of acidified skim milks and infant formulae made from cow and goat milk. Food Hydrocolloids, 2019, 96, 161-170.	5.6	41
22	Hierarchical self-assembly of a striped gyroid formed by threaded chiral mesoscale networks. Proceedings of the National Academy of Sciences of the United States of America, 2014, 111, 1271-1276.	3.3	40
23	Structural Evolution of Wormlike Micellar Fluids Formed by Erucyl Amidopropyl Betaine with Oil, Salts, and Surfactants. Langmuir, 2016, 32, 12423-12433.	1.6	39
24	Wormlike micelle formation of novel alkyl-tri(ethylene glycol)-glucoside carbohydrate surfactants: Structure–function relationships and rheology. Journal of Colloid and Interface Science, 2018, 529, 464-475.	5.0	38
25	Effect of amyloglucosidase hydrolysis on the multi-scale supramolecular structure of corn starch. Carbohydrate Polymers, 2019, 212, 40-50.	5.1	38
26	A novel lyotropic liquid crystal formed by triphilic star-polyphiles: hydrophilic/oleophilic/fluorophilic rods arranged in a 12.6.4. tiling. Physical Chemistry Chemical Physics, 2011, 13, 3139-3152.	1.3	36
27	Tricontinuous mesophases of balanced three-arm â€~star polyphiles'. Soft Matter, 2009, 5, 2782.	1.2	35
28	Polycontinuous geometries for inverse lipid phases with more than two aqueous network domains. Faraday Discussions, 2013, 161, 215-247.	1.6	35
29	Structural evolution of photocrosslinked silk fibroin and silk fibroin-based hybrid hydrogels: A small angle and ultra-small angle scattering investigation. International Journal of Biological Macromolecules, 2018, 114, 998-1007.	3.6	35
30	Chelating oleyl-EDTA amphiphiles: self-assembly, colloidal particles, complexation with paramagnetic metal ions and promise as magnetic resonance imaging contrast agents. Soft Matter, 2011, 7, 10994.	1.2	31
31	Polymeric Ionic Liquid Nanoparticle Emulsions as a Corrosion Inhibitor in Anticorrosion Coatings. ACS Omega, 2016, 1, 29-40.	1.6	31
32	Investigation of the micro- and nano-scale architecture of cellulose hydrogels with plant cell wall polysaccharides: A combined USANS/SANS study. Polymer, 2016, 105, 449-460.	1.8	31
33	Chemical delithiation and exfoliation of <mml:math xmlns:mml="http://www.w3.org/1998/Math/MathML" altimg="si0033.gif" overflow="scroll"><mml:msub><mml:mrow><mml:mi>Li</mml:mi></mml:mrow><mml:mrow><mml:mi>xlournal of Solid State Chemistry, 2014, 220, 102-110.</mml:mi></mml:mrow></mml:msub></mml:math 	nl:mi>4/mn	nl:mrow>
34	Nanoassemblies of Gd–DTPA–monooleyl and glycerol monooleate amphiphiles as potential MRI contrast agents. Journal of Materials Chemistry B, 2014, 2, 1225.	2.9	25
35	Gadolinium-DTPA amphiphile nanoassemblies: agents for magnetic resonance imaging and neutron capture therapy. Biomaterials Science, 2014, 2, 924-935.	2.6	24
36	Using SANS with Contrast-Matched Lipid Bicontinuous Cubic Phases To Determine the Location of Encapsulated Peptides, Proteins, and Other Biomolecules. Journal of Physical Chemistry Letters, 2016, 7, 2862-2866.	2.1	23

#	Article	IF	CITATIONS
37	Interfacial Structures of Droplet-Stabilized Emulsions Formed with Whey Protein Microgel Particles as Revealed by Small- and Ultra-Small-Angle Neutron Scattering. Langmuir, 2019, 35, 12017-12027.	1.6	22
38	PEGylation and surface functionalization of liposomes containing drug nanocrystals for cell-targeted delivery. Colloids and Surfaces B: Biointerfaces, 2019, 182, 110362.	2.5	22
39	Investigating linear and nonlinear viscoelastic behaviour and microstructures of gelatin-multiwalled carbon nanotube composites. RSC Advances, 2015, 5, 107916-107926.	1.7	21
40	Nanostructure of cokes. International Journal of Coal Geology, 2018, 188, 112-120.	1.9	21
41	H2O/D2O Contrast Variation for Ultra-Small-Angle Neutron Scattering to Minimize Multiple Scattering Effects of Colloidal Particle Suspensions. Colloids and Interfaces, 2018, 2, 37.	0.9	20
42	Structure Analysis of Solid Lipid Nanoparticles for Drug Delivery: A Combined USANS/SANS Study. Particle and Particle Systems Characterization, 2019, 36, 1800359.	1.2	20
43	A Bicontinuous Mesophase Geometry with Hexagonal Symmetry. Langmuir, 2011, 27, 10475-10483.	1.6	19
44	Sulfonated Thiophene Derivative Stabilized Aqueous Poly(3-hexylthiophene):Phenyl-C ₆₁ -butyric Acid Methyl Ester Nanoparticle Dispersion for Organic Solar Cell Applications. ACS Applied Materials & Interfaces, 2018, 10, 44116-44125.	4.0	18
45	Pore accessibility and trapping of methane in Marcellus Shale. International Journal of Coal Geology, 2021, 248, 103850.	1.9	18
46	Design and synthesis of an azobenzene–betaine surfactant for photo-rheological fluids. Journal of Colloid and Interface Science, 2021, 594, 669-680.	5.0	17
47	An attempt to detect bicontinuity from SANS data. Journal of Colloid and Interface Science, 2007, 312, 59-67.	5.0	16
48	Evaluation of Gd-DTPA-Monophytanyl and Phytantriol Nanoassemblies as Potential MRI Contrast Agents. Langmuir, 2015, 31, 1556-1563.	1.6	16
49	Structural and rheological changes of lamellar liquid crystals as a result of compositional changes and added silica nanoparticles. Physical Chemistry Chemical Physics, 2018, 20, 16592-16603.	1.3	15
50	Structural evolution of iron forming iron oxide in a deep eutectic-solvothermal reaction. Nanoscale, 2021, 13, 1723-1737.	2.8	14
51	Chelating DTPA amphiphiles: ion-tunable self-assembly structures and gadolinium complexes. Physical Chemistry Chemical Physics, 2012, 14, 12854.	1.3	13
52	Minimal nets and minimal minimal surfaces. Acta Crystallographica Section A: Foundations and Advances, 2013, 69, 483-489.	0.3	13
53	Worm-like micelles and vesicles formed by alkyl-oligo(ethylene glycol)-glycoside carbohydrate surfactants: The effect of precisely tuned amphiphilicity on aggregate packing. Journal of Colloid and Interface Science, 2019, 547, 275-290.	5.0	13
54	Gdâ€DTPAâ€Dopamineâ€Bisphytanyl Amphiphile: Synthesis, Characterisation and Relaxation Parameters of the Nanoassemblies and Their Potential as MRI Contrast Agents. Chemistry - A European Journal, 2015, 21, 13950-13960.	1.7	12

#	Article	IF	CITATIONS
55	Biomimetic Gemcitabine–Lipid Prodrug Nanoparticles for Pancreatic Cancer. ChemPlusChem, 2020, 85, 1283-1291.	1.3	12
56	Small angle neutron scattering quantifies the hierarchical structure in fibrous calcium caseinate. Food Hydrocolloids, 2020, 106, 105912.	5.6	12
57	The Tricontinuous 3ths(5) Phase: A New Morphology in Copolymer Melts. Macromolecules, 2014, 47, 7424-7430.	2.2	11
58	Fingerprint of hydrocarbon generation in the southern Georgina Basin, Australia, revealed by small angle neutron scattering. International Journal of Coal Geology, 2018, 186, 135-144.	1.9	11
59	Small-angle X-ray scattering (SAXS) and small-angle neutron scattering (SANS) study on the structure of sodium caseinate in dispersions and at the oil-water interface: Effect of calcium ions. Food Structure, 2022, 32, 100276.	2.3	10
60	Protein-Eye View of the in Meso Crystallization Mechanism. Langmuir, 2019, 35, 8344-8356.	1.6	9
61	Deformation of pores in response to uniaxial and hydrostatic stress cycling in Marcellus Shale: Implications for gas recovery. International Journal of Coal Geology, 2021, 248, 103867.	1.9	9
62	Nanocompartmentalization of Soft Materials with Three Mutually Immiscible Solvents: Synthesis and Self-Assembly of Three-Arm Star-Polyphiles. Chemistry of Materials, 2015, 27, 857-866.	3.2	8
63	Structural relationships for the design of responsive azobenzene-based lyotropic liquid crystals. Physical Chemistry Chemical Physics, 2020, 22, 4086-4095.	1.3	8
64	Tracking the heat-triggered phase change of polydopamine-shelled, perfluorocarbon emulsion droplets into microbubbles using neutron scattering. Journal of Colloid and Interface Science, 2022, 607, 836-847.	5.0	8
65	KOOKABURRA: The Ultra-Small-Angle Neutron Scattering Instrument at ANSTO. Neutron News, 2016, 27, 30-32.	0.1	7
66	<i>In Situ</i> Nanostructural Analysis of Concentrated Wormlike Micellar Fluids Comprising Sodium Laureth Sulfate and Cocamidopropyl Betaine Using Small-Angle Neutron Scattering. Langmuir, 2020, 36, 14296-14305.	1.6	7
67	Effect of porous waxy rice starch addition on acid milk gels: Structural and physicochemical functionality. Food Hydrocolloids, 2020, 109, 106092.	5.6	7
68	Exploring the transition of polydopamine-shelled perfluorohexane emulsion droplets into microbubbles using small- and ultra-small-angle neutron scattering. Physical Chemistry Chemical Physics, 2021, 23, 9843-9850.	1.3	7
69	Rearrangement in Brown Coal Microstructure upon Drying As Measured by Ultrasmall-Angle Neutron Scattering. Energy & Fuels, 2017, 31, 231-238.	2.5	6
70	Optimal packings of three-arm star polyphiles: from tricontinuous to quasi-uniformly striped bicontinuous forms. Interface Focus, 2017, 7, 20160130.	1.5	6
71	Investigation of the siliceous hydrogel phase formation in glass-ionomer cement paste. Physica B: Condensed Matter, 2018, 551, 287-290.	1.3	6
72	Determining the Hydration in the Hydrophobic Layer of Permeable Polymer Vesicles by Neutron Scattering. Macromolecules, 2020, 53, 7546-7551.	2.2	6

#	Article	IF	CITATIONS
73	Effect of red blood cell shape changes on haemoglobin interactions and dynamics: a neutron scattering study. Royal Society Open Science, 2020, 7, 201507.	1.1	6
74	Small-angle neutron scattering reveals basis for composition dependence of gel behaviour in oleic acid - sodium oleate oleogels. Innovative Food Science and Emerging Technologies, 2021, 73, 102763.	2.7	6
75	How to avoid multiple scattering in strongly scattering SANS and USANS samples. Fuel, 2022, 325, 124957.	3.4	6
76	Tuning the structure, thermal stability and rheological properties of liquid crystal phases via the addition of silica nanoparticles. Physical Chemistry Chemical Physics, 2019, 21, 25649-25657.	1.3	5
77	Structural Polymorphism of Resorcinarene Assemblies. Langmuir, 2020, 36, 6222-6227.	1.6	5
78	Polycation radius of gyration in a polymeric ionic liquid (PIL): the PIL melt is not a theta solvent. Physical Chemistry Chemical Physics, 2022, 24, 4526-4532.	1.3	5
79	Accessibility of Pores to Methane in New Albany Shale Samples of Varying Maturity Determined Using SANS and USANS. Energies, 2021, 14, 8438.	1.6	5
80	Towards advanced paramagnetic nanoassemblies of highly ordered interior nanostructures as potential MRI contrast agents. New Journal of Chemistry, 2017, 41, 2735-2744.	1.4	4
81	Membrane Protein Structures in Lipid Bilayers; Small-Angle Neutron Scattering With Contrast-Matched Bicontinuous Cubic Phases. Frontiers in Chemistry, 2020, 8, 619470.	1.8	4
82	Crystallographic characterization of fluorapatite glass-ceramics synthesized from industrial waste. Powder Diffraction, 2017, 32, S61-S65.	0.4	3
83	Micron-scale restructuring of gelling silica subjected to shear. Journal of Colloid and Interface Science, 2019, 533, 136-143.	5.0	3
84	Self-Assembly of Surfactin into Nanofibers with Hydrophilic Channels in Nonpolar Organic Media. Langmuir, 2020, 36, 7627-7633.	1.6	3
85	Structure–Performance Relationships for Tail Substituted Zwitterionic Betaine–Azobenzene Surfactants. Langmuir, 2022, 38, 7522-7534.	1.6	3
86	Formation and Characterization of Emulsified Microemulsions. Surfactant Science, 2008, , .	0.0	2
87	Small Angle Neutron Scattering Study of a Gehlenite-Based Ceramic Fabricated from Industrial Waste. Solid State Phenomena, 2019, 290, 22-28.	0.3	1
88	Texture Effects in the Delithiation of Lithium Cobalt Oxide. Materials Science Forum, 2012, 736, 301-306.	0.3	0
89	Microstructure characterisation through ultra-small-angle neutron scattering. International Journal of Nanotechnology, 2018, 15, 766.	0.1	Ο